Journal of Molecular Graphics and Modelling 49 (2014) 55–67

Contents lists available at ScienceDirect

Journal of Molecular Graphics and Modelling

journal homepage: www.elsevier.com/locate/JMGM

Stereoselective propagation in free radical polymerization of acrylamides: A DFT study

Gülru Kayık, Nurcan Ş. Tüzün*

Chemistry Department, Istanbul Technical University, Faculty of Science and Letters, Ayazaga Campus, Maslak, Istanbul, Turkey

ARTICLE INFO

Article history:
Accepted 8 January 2014
Available online 19 January 2014

Keywords:
Stereoselective
Radical polymerization
Acrylate
DFT
Pro-racemo
Pro-meso

ABSTRACT

In this study stereospecific free radical polymerization of *N*,*N*-alkylamides [*N*,*N*-dimethylacrylamide (DMAAm), *N*-methyl-*N*-phenylacrylamide (MphAAm) and *N*,*N*-diphenylacrylamide (DPAAm)] is investigated with density functional theory (DFT) calculations. Model propagation reactions at dimeric stage are used to elucidate the effect of substituent bulkiness, temperature and solvent polarity on stereospecific addition modes. In calculations all the monomers favor gauche conformation in their pro-meso and pro-racemo additions in general. The DFT calculations have reproduced the stereospecificity seen in these monomers. The implicit solvent calculations performed with IEFPCM have further refined the quantitative agreement. The calculations of DMAAm in solvents of different polarity (toluene, THF, chloroform and 2-propanol) have successfully reproduced the experimental trend both qualitatively and quantitatively. Tartrate molecules as stereospecifity inducer in DMAAm are considered and the experimentally observed change in stereospecificity from iso to syn in their presence have been elucidated by modeling the possible orientations of transition states in the propagation step. The favorable stereospecific addition modes are explained via interplay between the steric effects and the hydrogen bonding interactions.

1. Introduction

Free radical polymerization (FRP) is one of the most important and widely used techniques to obtain polymers due to its applicability to wide range of monomers, relative cheapness and the easiness of the process. Tacticity control in free radical polymerization is an important topic since it affects the properties of end-products such as the mechanical strength, the melting and glass transition temperatures or solubility. However, most of the polymers produced by free-radical polymerization lack tacticity and are mostly atactic polymers. The structure of the propagating polymer chains makes it hard to control the stereospecific addition mode of the polymerization reaction because the sp^2 planar propagating radical species do not efficiently control the addition mode as compared to ionic or coordination polymerizations. Experimental works reveal that in order to control the stereospecificity of free radical polymerization, reaction conditions such as temperature, solvent, monomer/initiator ratio or stereospecificity additives should be regulated since they all affect the tacticity of the polymer.

Quantum mechanical calculations have been employed in polymer area as well as in other applications of chemistry. Especially, many studies have helped in understanding the steps of reactions by concentrating on kinetics as well as thermodynamics of FRP reactions [1–12]. Calculations also give chance to investigate the steric and electronic effects of substituents, solvent, temperature and stereospecific additives on the energy barriers of the different stages of the reactions individually. Quantum chemical calculations is also an advantageous way to study the tacticity phenomenon comprehensively because it enables to explore all of the possible addition modes of the monomer to the propagating radical together, which is the origin of stereoselective propagation in these polymeric systems. The difference between the activation barriers for the addition to the diastereotopic faces of the radical with the propagating chains determines the selectivity of the propagation reaction. In the literature, there are many studies that successfully use quantum mechanical procedures to investigate stereoselectivity in the propagation step of free radical polymerization of various polymers [13–16]. These studies have accounted on the modes of addition that control tacticity and the effects of substituents on them. In one of those studies [13], the tacticities of methylacrylate (MA) and methyl methacrylate (MMA) have also been modeled with density functional theory using B3LYP/6-31+G(d) basis set for calculating the reaction barriers for the iso and syn additions. The reported results have shown qualitative agreement with the experimental finding that both of the monomers favor syndiotactic addition over the isotactic one. Another study [14] on the solvent effect of methyl methacrylate in its stereospecific polymerization have revealed that using methanol and $(CF_3)_3COH$ as a solvent

* Corresponding author. Tel.: +90 212 2853163.
E-mail address: nurcant@itu.edu.tr (N.Ş. Tüzün).

1093-3263/$ – see front matter © 2014 Elsevier Inc. All rights reserved.
http://dx.doi.org/10.1016/j.jmgm.2014.01.005

has yielded syndiotactic rich polymer due to the hydrogen bond formation between the carbonyl oxygen of the monomer and alcohol's hydrogen in the transition structures. Stabilizing effect of the $(CF_3)_3COH$ on the transition structures has been attributed to the relatively higher steric effect of the solvent molecules and stronger hydrogen bond formation as compared to methanol as solvent. In another study, the tacticity of *N*-isopropylacrylamide (NIPAAm) was modeled to understand the solvent effect [15].

Experimental studies revealed that free radical polymerization of *N*,*N*-dimethylacrylamide (DMAAm) gives isotactic rich polymer in various reaction conditions. For example Hirano et al. obtained isotactic rich polymer in toluene at low temperatures [17]. They found that at −80 °C poly(DMAAm) has m/r ratio of 73/27. However, it was found that syndiotactic rich polymer is favored in the case of *N*-methyl-*N*-phenylacrylamide (MphAAm) [18] and *N*,*N*-diphenylacrylamide (DPAAm) [18,19] in similar experimental conditions.

In this study, we focus on the tacticity of a series of *N*,*N*-alkylacrylamide monomers in their free radical polymerization reactions. We have investigated all the possible addition modes of various acrylamides in their propagation step of free radical polymerization to account on their stereospecificity with quantum chemical tools. For this purpose, three different substituted acrylamides, *N*,*N*-dimethylacrylamide (DMAAm), *N*-methyl-*N*-phenylacrylamide (MphAAm) and *N*,*N*-diphenylacrylamide (DPAAm) have been studied (Fig. 1). The effects of substituent, solvent and temperature on the stereospecific addition modes in free radical polymerization of these aforementioned acrylamides have been elucidated. Experiments on the free radical polymerization of DMAAm by Hirano et al. have shown a change from isotactic to syndiotactic products when tartrate molecules are present in the reaction medium. In order to induce stereospecifity in free radical polymerization, Lewis acids and bases have been utilized many times [20–22]. Various phosphoric acid esters have been tested on NIPAAm and hydrogen bonding interaction between monomer–phosphate complexes were found to induce stereospecifity [22]. Another study also investigated the stereospecific polymerization of *N*-vinylacetamide by using Lewis acids and alcohol compounds in which they found the importance of hydrogen bonding formation between additives and monomers such that the tartrates, a diol, induced isotacticity in toluene at low temperatures [23]. The effect of 3,5-dimethylpyridine *N*-oxide as an isotacticity inducer in various solvents in FRP of *N*-methylacrylamide has been tested and shown [24]. In all these and unreferenced examples, the main procedure is to add ingredients that form H-bondings with monomer and/or polymeric fragments to induce synthesis of stereospecific polymers.

In this study we aim to model the propagation steps of free radical polymerization of a series of acrylamide monomers (Fig. 1) to elucidate the reasons of stereospecificity in their different addition modes.

2. Methodology

In this study, all calculations were performed with density functional theory by using Gaussian 09 program package [25]. Studying polymerization reactions require a reasonable method that is both cost effective and reliable because of the large size of the polymer systems that need a model to mimic the real system [26]. DFT is widely used in a huge number of computational studies involving similar systems, involving radical addition reactions; propagations, homopolymerizations, β-scission and chain transfer in free radical reactions [10,27–35].

B3LYP method with 6-31+G(d,p) basis set was chosen for geometry optimizations of monomers, radicals and transition state structures in the gas phase. Even though this methodology is less accurate in prediction of electronic energies, it is generally accepted that B3LYP methods provide excellent low cost performance especially in geometries. Non-systematic errors in DFT have also been reported in the literature [3,36]. However, these studies are concerned with predicting absolute rate constants, which are very sensitive to prediction of accurate activation energies and pre-exponential factors. Since we are not dealing with absolute rate constants in this study but rather interested in comparing the relative energy barriers of the two modes of addition in propagation reaction of a monomer with it radical (one gives arise to a meso and the other to racemo addition), B3LYP functional set which is known to yield satisfactory results especially for the geometries was used [9,10,13,34]. In the literature, energetics were recalculated by single point calculations with some other functionals such as M06X, BMK and MPW by making use of B3LYP geometries, based on the general agreement that B3LYP methods provide satisfactory low-cost performance for structure optimizations [10,13,32,37–39]. In this study, a series of benchmark calculations are performed with BMK [40], MPWB1K [41], M05-2X [42], M06-2X [43] and MP2 at 6-311+G(3df,2p) level of theory at the B3LYP/6-31+G(d,p) geometries. Those functionals are chosen since BMK is reported to have good performance in kinetics of radical reactions in general [11,31,44,45], MPWB1K in describing H-bondings and accurate thermochemical results [11,41,46], M06-2X [47] in thermochemistry and M05-2X [42,48] in describing radical species.

IRC calculations were also carried out to ensure that the correct transition state structures were found on the potential energy surface of propagation reactions. All possible conformers of the species have been searched carefully to ensure that the global minimum structures have been obtained and the B3LYP vibrational frequencies were used to characterize species as minima or transition states.

To include the solvent effect on the stereospecific addition mode of the propagating radical to the monomer, implicit solvation methodology is used without re-optimization of the gas phase geometries. For this purpose, the integral equation formalism model (IEF-PCM) which is one of the continuum solvation methods that include polar environment effects is utilized. In this method solvent is characterized by its dielectric constant ε and treated as a continuum medium around the solvated species [49]. This model is a self-consistent reaction field method which treats the solvent as a continuum of uniform dielectric constant by creating the solute cavity as a set of overlapping spheres. IEF-PCM methodology has been used to model the solvent effect on free radical polymerization of systems including various acrylates [10,14,47].

In order to understand the temperature and solvent effects on the addition modes, the Boltzmann distribution is used to obtain the relative population of transition state structures for pro-meso and pro-racemo additions as in literature [50]. In cases where there are multiple transition states within almost 2 kcal/mol relative energy, these are included in the distribution calculations as well. The results from these calculations are used to compare the with the experimental meso (m) and racemo (r) dyads ratio, including the level of theory calculations. In the solvent and temperature effect calculations only the most stable transition state has been used.

In the discussion that follows, all the energies in the gas phase are free energies at 25 °C and in solvent electronic energies unless otherwise stated. The zero of the reaction coordinate will be considered as the point of reactants at infinite separation and the radical addition barriers will be calculated accordingly.

3. Results and discussion

In free radical polymerization, the propagating radical attacks the monomer, breaks the C=C double bond of the monomer which

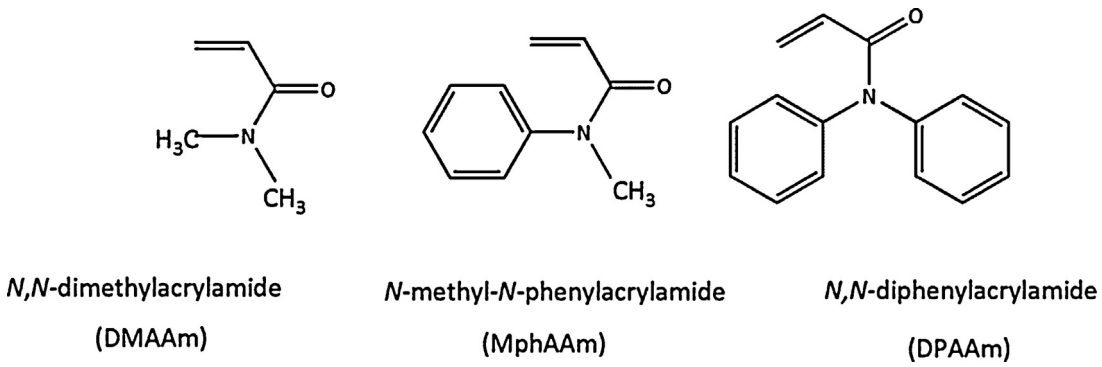

Fig. 1. Modeled monomers in this study.

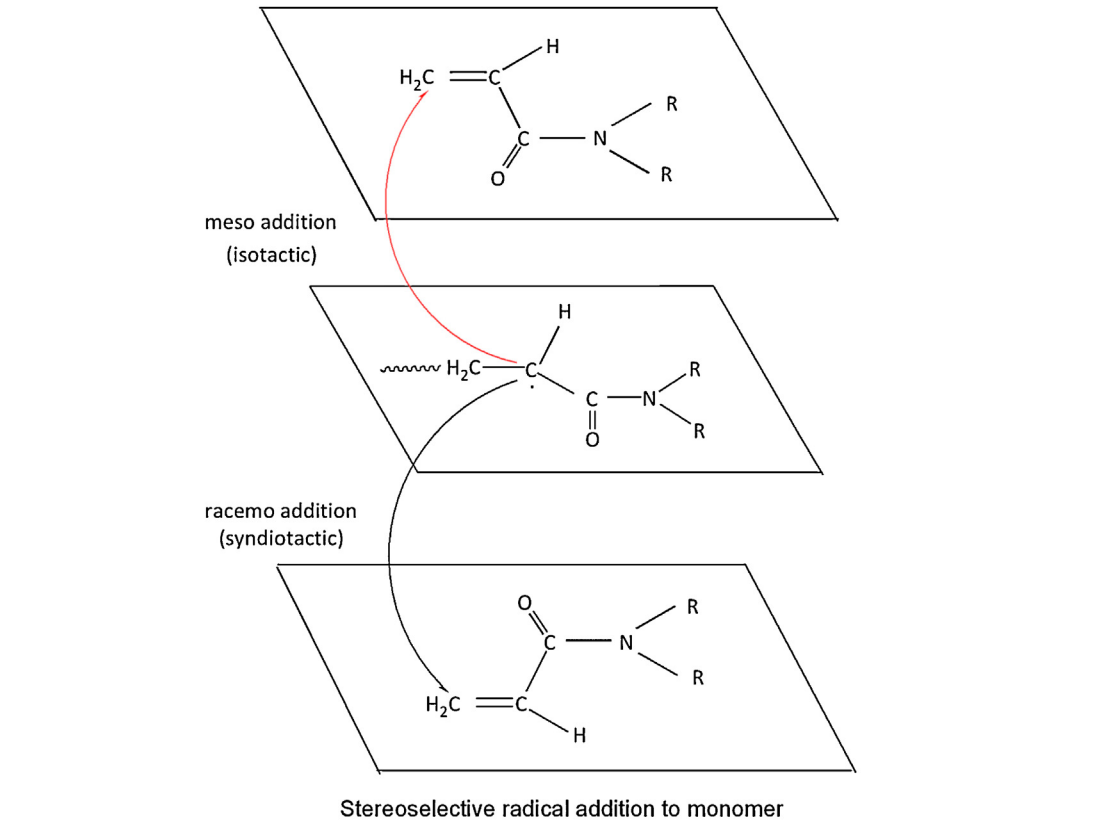

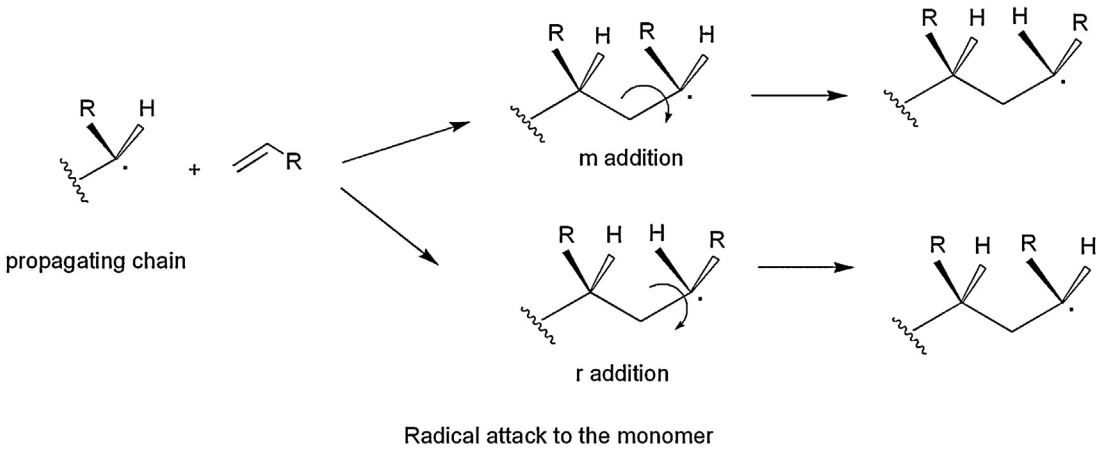

Fig. 2. Stereoselective propagation reaction in free radical polymerization.

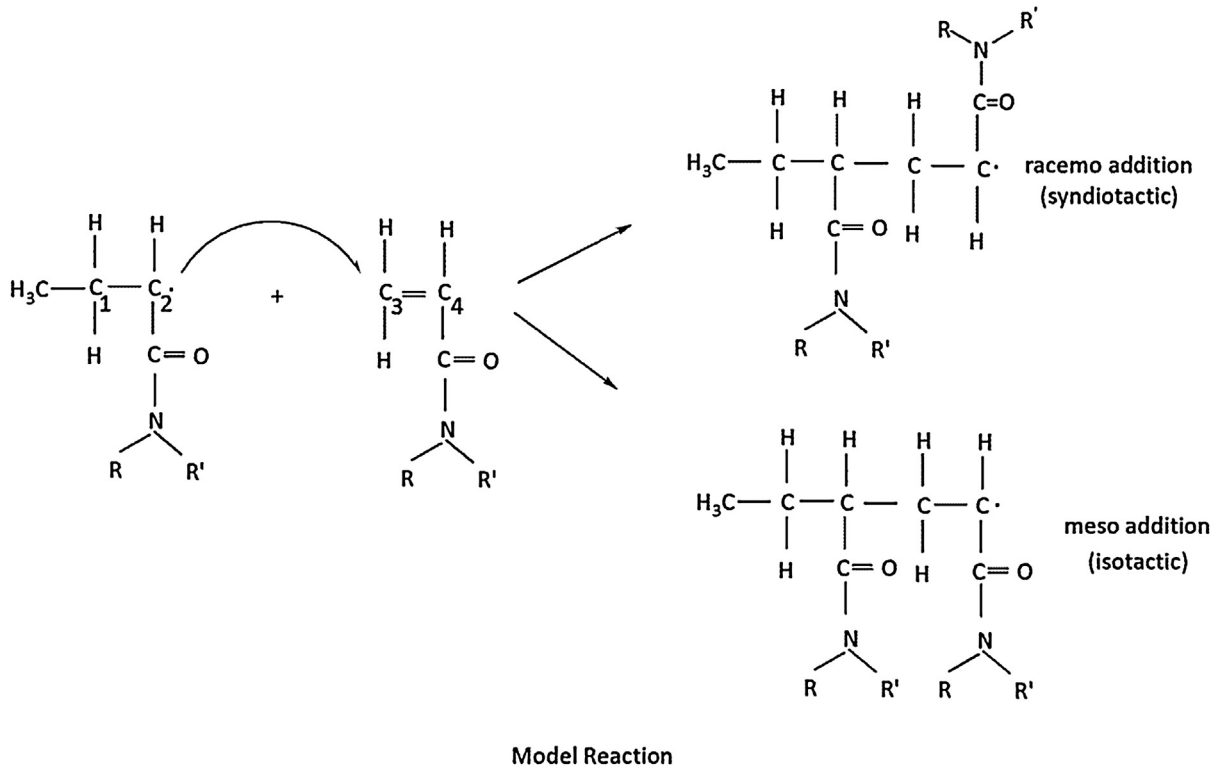

Fig. 3. Model reaction for the propagation step of free radical polymerization (θ dihedral angle is defined between the C1–C2–C3–C4).

then leads to generation of the new radical and this addition sequentially goes on until termination reactions occur. Tacticity refers to the stereoregularity in the configurations of successive stereocenters in a polymer chain. In the case of CH_2=CHR type vinyl monomers, there are two possible ways that a monomer could attach to a growing chain from two different faces of the growing radical which then gives possibility to form two different dyads: meso (m) and racemo dyads (Fig. 2).

In the coarse of our study only propagation has been modeled since it is the step that determines the mode of stereospecific addition. The propagation step was modeled at the dimeric stage (Fig. 3) and the stereoselectivity has been evaluated by considering the addition of unimeric radical to monomer. To consider dimers when modeling free radical homopolymerizations is an acceptable simplification because the penultimate unit is far away from the reaction center and its effects on the addition modes can be neglected when compared to the substituent that is attached to the ultimate monomeric unit. It has been reported that the number of fragments in the growing chain do not affect the activation barrier for the propagation reaction [51]. There are some other studies in the literature that validate this argument. For example, Coote et al. showed that, in free radical polymerization of acrylonitrile and vinylchloride, using trimers or longer chains have not done significant effect on the value of the rate constants [3].

In the model, methyl radical ($CH_3^{\bullet}$) is used to mimic the radical propagating chain (Fig. 3). In the literature, this methodology has been reported to be adequate for description of growing polymer radicals in radical polymerization reactions [47,50,52–60]. In calculations herein, all the possible addition modes have been considered for all types of conformations of the model propagating chain and the monomer.

In our model reaction (Fig. 3) we adopt the same assumption that in the propagation reaction, the addition is mostly directed by the interaction of the monomer and the ultimate monomeric unit of the radical rather than the penultimate unit. The attack of model propagating radical to the monomer may result in the formation of pro-meso or pro-racemo transition states which could in turn lead to racemo and meso dyads, respectively, by sequential addition of another monomer to the newly formed radical center at the ultimate monomeric unit. During radical polymerization, rotation around the terminal bond at the radicalic center may possibly take place before the addition of an incoming monomer (Fig. 2). However, we assume in this study that the stereoselectivity is mostly directed by the stereospecific addition to the two diastereotopic faces of the planar radicalic site at the experimental reaction temperature (−80 to 0 °C) [17,18] where rotation is presumably hindered.

The propagation reactions are modeled according to the head to tail regioselectivity which is known to be the favorable attachment due to the steric, resonance and inductive effects [31,61].

4. DMAAm (without tartrates)

The most stable conformers of *syn* and *anti* isomers of DMAAm and the corresponding monomeric radical are shown in Fig. 4. The most stable conformer DMAAm-syn has the C=O and C=C groups *syn* to each other as expected for acrylamides [62,63]. It has a planar shape where the nitrogen is almost sp^2 hybridized due to delocalization between the alkene, carbonyl and the lone pair of nitrogen. Although both *anti* and *syn* conformations are stabilized with intramolecular H-bondings, the *anti* geometry is 2.25 kcal/mol higher in energy than the *syn* conformer. The energy gap between the *syn* and *anti* geometries become higher in their corresponding radicalic monomers, implying a *syn* radicalic species to exist predominantly in the reaction medium.

Propagation step was modeled at the dimeric stage considering the most stable monomer (DMAAm-syn) (Fig. 4) and its corresponding radical (DMAAm-rad-syn) (Fig. 4) since the *anti* conformer of monomer is significantly higher in energy. Having considered all possible orientations and conformations for the

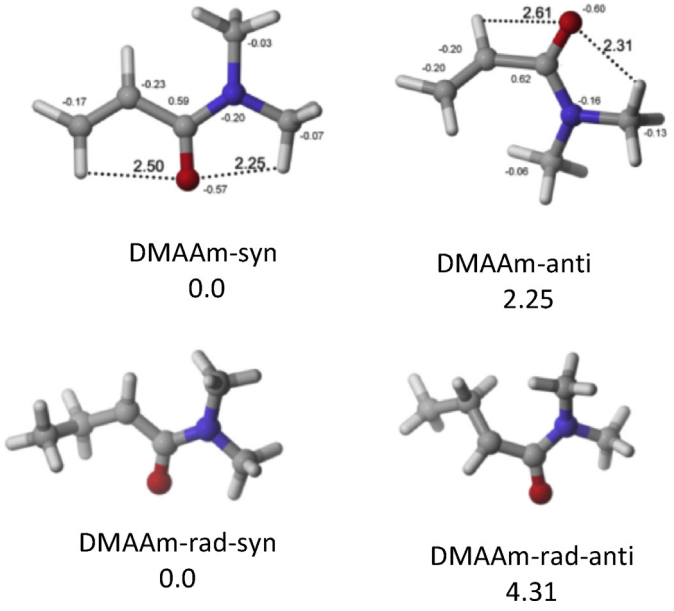

Fig. 4. The most stable conformers of DMAAm monomer and its radical (the relative free energies are in kcal/mol).

stereospecific addition, the obtained least energetic pro-racemo and pro-meso transition state structures within almost 2.0 kcal/mol of relative energy are depicted in Fig. 5.

The monomeric radical attacks to the monomer in a gauche fashion in the case of pro-meso addition (DMAAm-ts-iso1, $\theta = -70.1^{\circ}$) whereas, in pro-racemo addition, a trans conformation of the backbone (DMAAm-ts-syn1), leading to a torsion angle θ of -168.1° is preferred (Fig. 5). The second higher energy transition states for both pro-meso and pro-racemo additions are gauche with $\theta = 60.2^{\circ}$ and $\theta = -84.3^{\circ}$, respectively.

Gauche addition is the most favorable addition mode in the free radical polymerization in most of the cases. For example, in the addition of n-alkyl radicals to ethylene, calculations show that gauche addition is favored over the trans conformation [6]. In another quantum chemical study, addition of γ-substituted propyl radicals to various alkenes have shown that the lowest energy transition structures were the conformations with gauche attachments [64]. The methyl acrylate and vinyl acetate free radical propagation reaction [4], studied theoretically at dimeric stage has shown that the gauche addition was also the preferred mode of attack, in which hydrogen bonding is playing critical role in stabilizing the crowded conformation in gauche additions. Similar effects on the stereoselectivity of free radical polymerization of the methyl acrylate (MA), methyl methacrylate (MMA) and *N*-isopropylacrylamide (NIPAAm) monomers are shown in the literature [13,65–67]. In these studies, gauche orientation was preferred in pro-meso addition mode in all cases with MMA, MA and NIPAAm. However, in pro-racemo addition, the trend changes and may be trans or gauche depending on the nature of the reacting monomers: In MA and NIPAAm, the orientation is trans whereas in MMA gauche is preferred. These preferences are reported to be due to two factors. (i) Steric repulsions between the reacting fragments; (ii) H-bondings. The importance of hydrogen bonding interaction is pointed out in these studies such that the interaction between the C=O and N—H or CH_3 groups determine the conformation of the main chain of the polymer and also it is shown that the dimers having intramolecular hydrogen bondings are more stable than the ones which do not have when the backbone of the polymers have the same conformation [66,67].

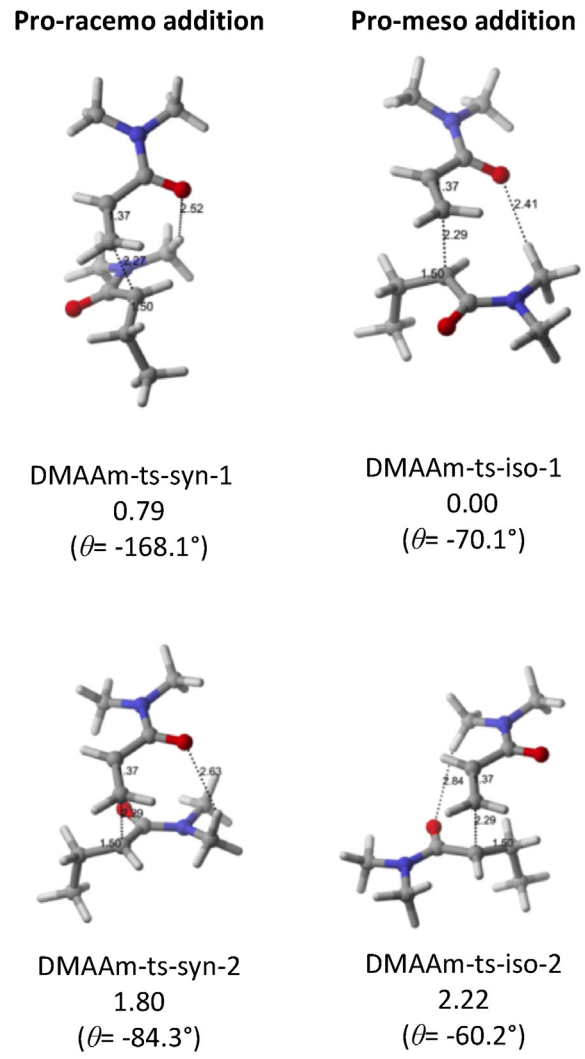

Fig. 5. The transition state structures for pro-racemo and pro-meso additions of DMAAm (the relative free energies are in kcal/mol).

Likewise, in addition to the preserved intramolecular H-bondings in monomeric fragments, in the least energetic pro-meso (isotactic) and pro-racemo (syndiotactic) transition state structures, hydrogen bonding interactions between the reacting fragments (at 2.52 Å and 2.41 Å in DMAAm-ts-syn-1 and DMAAm-ts-iso-1, respectively) are built up (Fig. 5). Although both N and O of C=O group are potent H-bond donors, oxygen is mainly responsible for H-bondings since the sp^2-like nitrogen is protected by pendant methyl groups and is not prone to form H-bonding interactions. Comparing the pro-racemo and pro-meso additions within their possible geometries, the transition states with the same backbone configuration which allows stronger H-bondings are more stable. For example, in two gauche pro-meso addition transition state structures, DMAAm-ts-iso-1 has a stabilizing interaction of 2.41 Å whereas DMAAm-ts-iso-2, with relatively 2.22 kcal/mol higher energy, has 2.84 Å for the same interatomic distance. Apart from the steric effects, the weaker hydrogen bonding interactions in the second least energetic transition structures (DMAAm-ts-syn-2 and DMAAm-ts-iso-2) (Fig. 5) strengthens this suggestion. These interactions are important factors for stabilizing the structures and determination of the stereoregularity in the product. In the most stable addition transition structure (DMAAm-ts-iso-1) there is an interplay between the steric hindrances and H-bondings.

Table 1
The calculated and experimental m:r ratios for DMAAm polymers with and without tartrate at a series of temperature.

Temperature (°C)	Without tartrate		With tartrate	
	m:r ratioExperimental[a]	m:r ratioB3LYP	m:r ratioExperimental[a]	m:r ratioB3LYP
0	62:38	81:19	46:54	41:59
−20	64:32	84:16	43:57	39:61
−40	66:34	86:14	40:60	38:62
−60	70:30	88:12	37:63	36:64
−80	73:27	91:9	37:63	34:66

[a] Ref. [17].

In the calculations performed herein, DMAAm prefers pro-meso over pro-racemo addition with 0.79 kcal/mol, in agreement with the experimental findings [17]. In that study, DMAAm is polymerized in toluene at low temperatures and found to yield m/r ratio of 62:38 in toluene at 0 °C which is calculated as 79:21 from Boltzmann distribution of transition states. Considering only the lowest energy transition states lead to only a slight change in distribution (81:19) (Table 1).

The effect of temperature was also investigated by Hirano et al. The calculated m/r ratio (Table 1) is in accordance with the trend observed in the experiments. In both experiments and calculations, as the temperature decreases, isotactic addition becomes more favorable. This can be attributed to the fact that as the temperature decreases, the backbone of the polymer chain mobility decreases and this restriction causes the syn addition being more difficult at low temperatures as it is already less favored at 25 °C. Although the quantitative agreement with the experiment is not perfect, the experimental trend is reproduced and the predominance of isotactic product is shown (Table 1).

Solvent effects can be understood by exploring the reaction kinetics as it changes the propagation rate constants of polymerization reactions especially in the case of water soluble monomers. For instance, acrylic acid [12] and acrylamides [11] show large variations with use of various solvents depending on the polarity and the nature of the intermolecular interactions that is formed between the monomer and the solvent.

Solvent effect on the stereospecificity of the radical polymerization is also known from experiments [19,20] and quantum chemical studies [14]. Many specific solvents have been found to allow stereospecific radical polymerizations via various interactions with monomers [68].

In the experimental works [19,69] solvent effect on tacticity of DMAAm was investigated explicitly including toluene, THF, 2-propanol and chloroform at different temperatures with different monomer and initiator ratios. A concentration effect was observed experimentally. In our study, the data belonging to the same monomer:initiator concentration ratios were used for comparative purposes. A relationship between the solvent polarity and the tacticity was obtained in that work such that increasing the polarity caused decrease in the isotacticity in polymers. Although the solvent methodology employed here do not consider specific solute–solvent interactions, the calculated m:r ratio reflected the experimental trend (Table 2). Furthermore, the quantitative trend has also improved in solvent calculations. As the dielectric constant of solvent increases, the pro-racemo addition becomes more favorable. This trend is reflected in our calculations, by the barrier of propagation reaction becoming smaller in pro-racemo mode of addition.

5. DMAAm (with tartrates)

Different tartrate molecules (diethyl L-tartrate, diisopropyl L-tartrate and di-*n*-butyl L-tartrate) were used as syndiotacticity inducer in free radical polymerization of DMAAm in toluene at temperatures ranging from 0 °C to −80 °C by Hirano et al. [17]. In the experimental study [17] it was proposed that there exists a complex formation between tartrate molecules and the monomeric species through hydrogen bonding interactions that affect the stereospecificity of the polymerization by increasing the tendency to form r dyads.

The experimentalists have expected three different complexes between the monomer and the tartrate molecules (Fig. 6).

To account for the effect of tartrate in the polymerization of DMAAm, calculations are performed in this study. The minimum energy structures for tartrates (ethyl tartrate-1 and ethyl tartrate-2, respectively) (Fig. 7) were located by scanning their potential energy surfaces.

In the minimum energy conformer of tartrates, the two hydroxyl and carbonyl groups are located on the same side creating very effective H-bondings that stabilize the system. From the minimum energy conformer of ethyltartrate (ethyl tartrate-1), monomer–tartrate complexes proposed by the experimentalists are modeled. Calculations show that, in the lowest energy monomer–tartrate complex (Fig. 8), tartrate has two hydroxyl groups located on the same side with two intramolecular hydrogen bondings, providing an extra stabilization to this conformer.

This result is in agreement with the predictions of the experimental work [17] and also other works conducted by Polavarapu et al. [70] and Buffeteau et al. [71]. 2:1 complex is slightly more favorable (0.61 kcal/mol) than 1:1 complexes in terms of electronic energy but when entropy effects are included, 1:1 complex with double hydrogen bond is more favorable in terms of free energy. Thus, the propagation reaction is modeled with this complex and the radical form of monomer complexed with this tartrate as in 1:1 complex with double hydrogen bond. At this stage, due to the necessity of saving time and computer resources, ethyl group in tartrate has been modified such that the terminal $-OCH_2CH_3$ parts have been replaced with a proton. The most stable conformer of

Table 2
The calculated and the experimental m:r ratios of DMAAm in various solvents.

Temperature (°C)	Solvent	Dielectric constant of the solvent	Calculated m:r ratio	Experimentalm:r ratio
−80	Toluene	2.38	74:26	73:27[a]
−60	Chloroform	4.81	63:37	70:30[b]
−78	THF	7.5	56:44	62:38[a]
−78	2-Propanol	18	51:49	57:43[a]

[a] Ref. [19].
[b] Ref. [69].

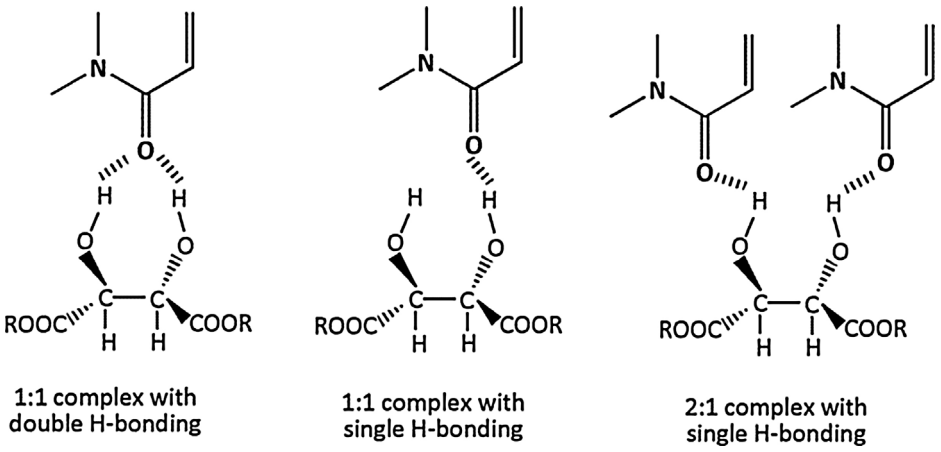

Fig. 6. Possible DMAAm monomer–tartrate complexes.

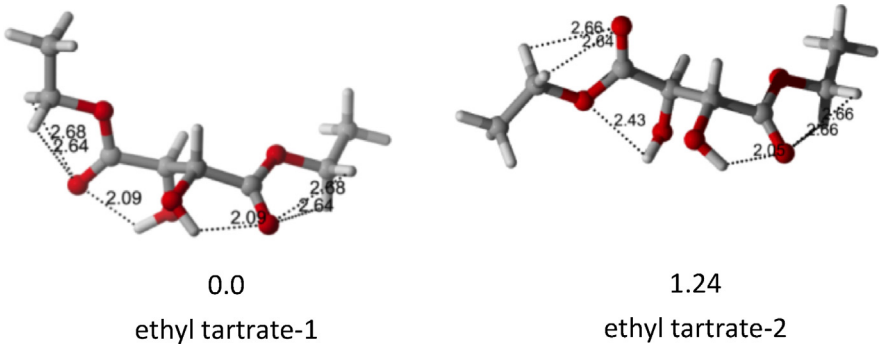

Fig. 7. The most stable ethyl tartrate molecules and some of H-bondings in these structures (the relative free energies are in kcal/mol).

this model tartrate has got the same backbone structure and OH group orientations as in ethyltartrate–monomer complex (Fig. 9).

The propagation reaction has been modeled with monomer–model tartrate (DMAAm-complex) and radicalic monomer–model tartrate (DMAAm-rad-complex) complexes to account on their stereospecific additions (Fig. 10).

In the pro-racemo addition, polymer backbone adopts trans conformation regardless of being with or without tartrate. This orientation of the backbone enables the formation of sterically unhindered geometry while the double hydrogen bondings between the tartrates and monomeric fragments are kept in the transition structure (DMAAm-ts-complex-syn1, Fig. 10). Additionally, the carbonyl groups on tartrates form very effective H-bondings with the monomeric fragments, adding stability to the system. As a result of these new H-bonding interactions, the H-bonds in the monomer–tartrate complexes become shorter. The next higher energy transition structure is with a relative energy of 0.99 kcal/mol (DMAAm-ts-complex-syn2) (Fig. 10) which has a very similar backbone geometry ($\theta = -152.97^{\circ}$) as that of minimum energy structure. The only difference is due to a change in the orientation of the tartrate and a small shift of θ angle ($\theta = -140.31^{\circ}$) which enables only one H-bonding between carbonyl oxygens and monomer fragments which were double in the lowest energy structure. Another transition state structure, DMAAm-ts-complex-syn3, which is 2.01 kcal/mol higher in energy than DMAAm-ts-complex-syn1 adopts a gauche conformation, where the steric repulsions

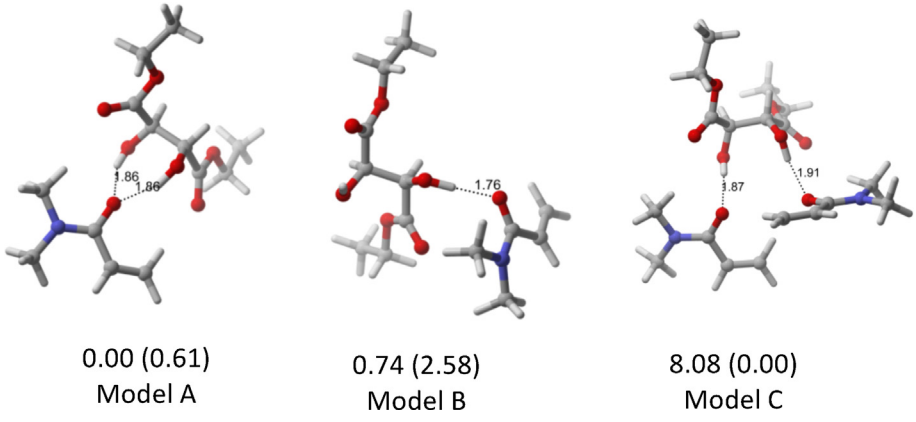

Fig. 8. The 3-dimensional geometries and the relative energies of possible monomer–tartrate complexes (the numbers in parentheses are relative electronic energies in kcal/mol).

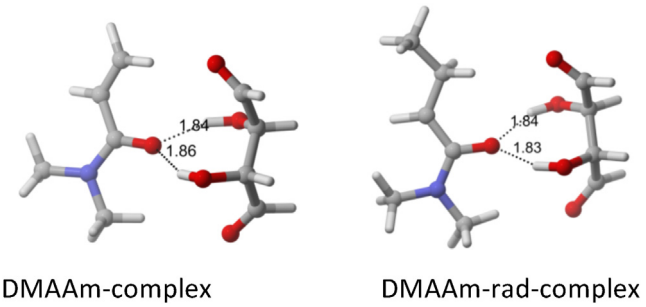

Fig. 9. The 3-dimensional geometries for the model tartrate–monomer and model tartrate–radicalic monomer complex.

are increased and the extent of H-bondings are decreased such that the two of the four terminal carbonyl oxygens can form only two weak interactions. The lowest energy transition structure has slightly shorter O—H distances for H-bondings coming from the monomer–tartrate complexes than their reactant counterparts. In pro-meso addition (DMAAm-ts-complex-iso1) although gauche orientation is preferred without tartrates, the presence of tartrates enforces a synperiplanar conformation in order to overcome the steric repulsions. The gauche conformation of the transition state would be 4.10 kcal/mol higher in electronic energy than the synperiplanar case (Fig. 11).

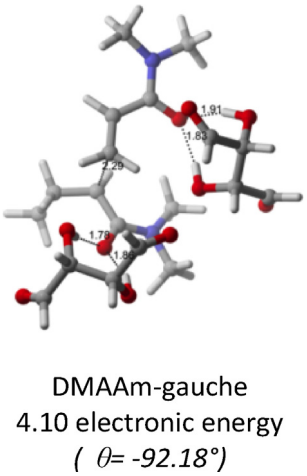

Fig. 11. The transition state structure of DMAAm in gauche fashion.

The transition state structures also demonstrate that due to the effective H-bondings between the carbonyl oxygens and the

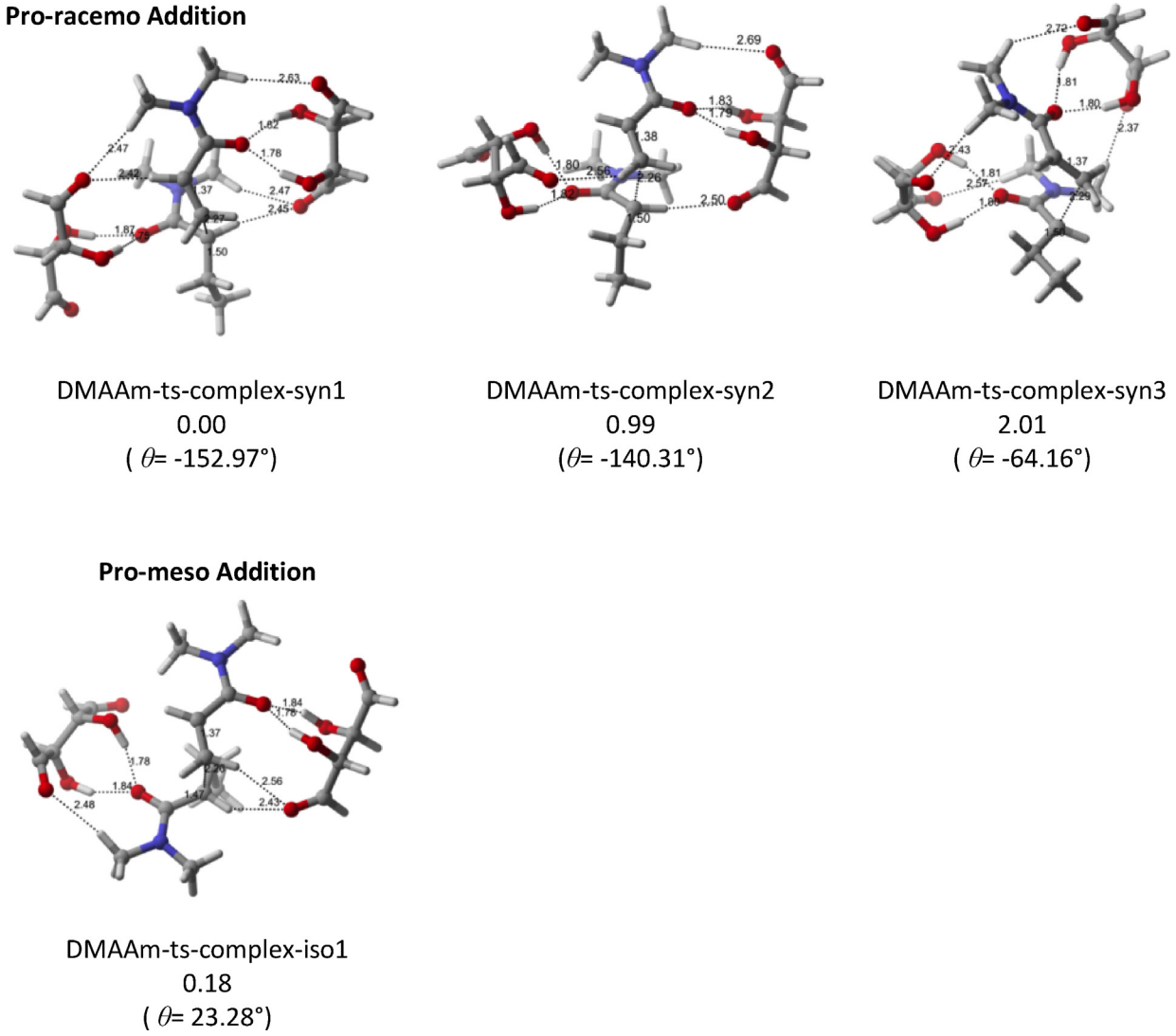

Fig. 10. The transition state structures for pro-racemo and pro-meso additions of DMAAm in the presence of tartrates (the relative free energies are in kcal/mol).

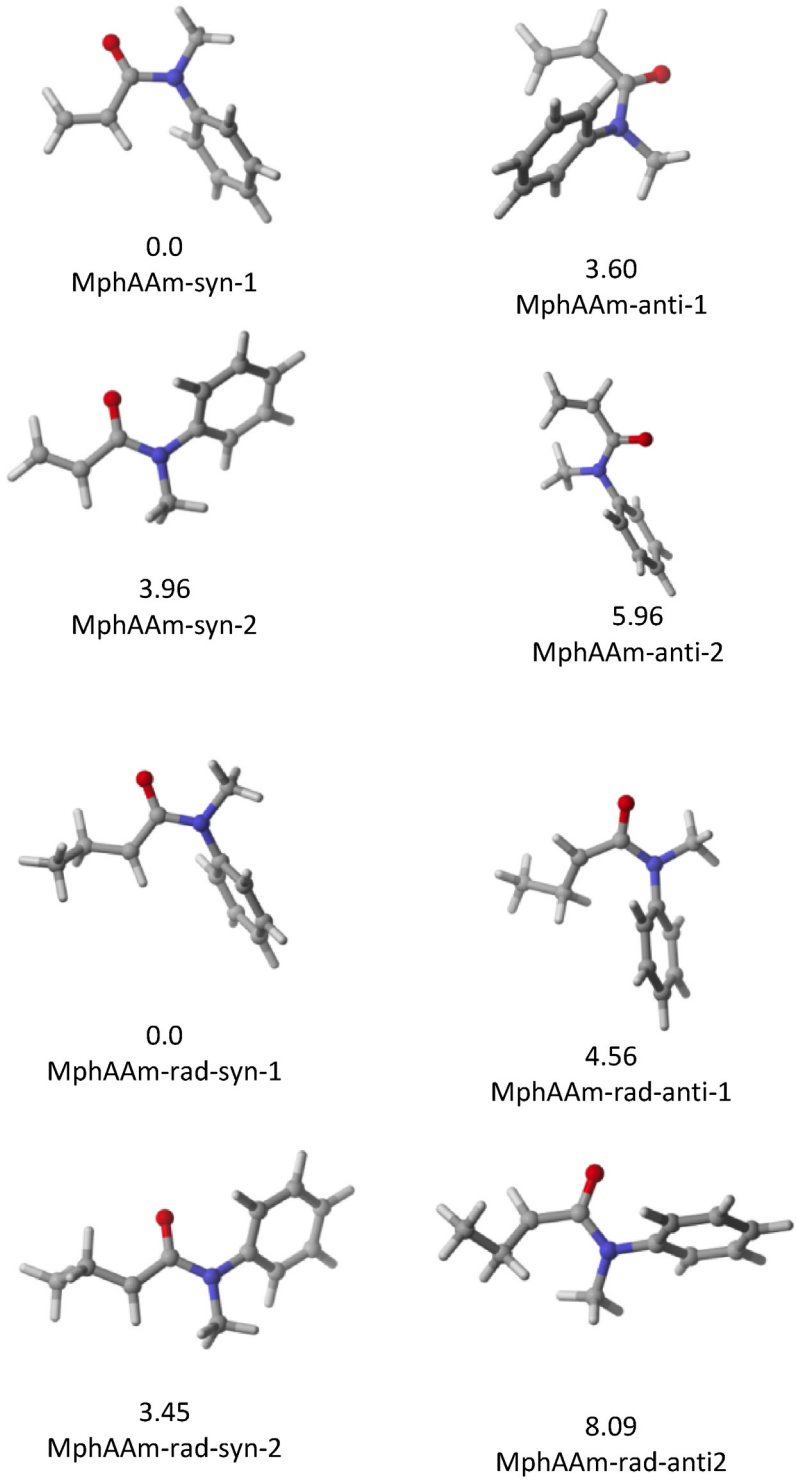

Fig. 12. The most stable conformers of MphAAm monomer and its radical (the relative free energies are in kcal/mol).

monomers, excluded R groups on tartrates would be away from the reaction center if they were present. Thus, an error stemming from this model is expected to be minimal.

The temperature effect was also examined in the presence of tartrates (Table 1). For DMAAm, at low temperatures, isotacticity was found to dominate whereas; the presence of tartrates was found to reverse the trend. The low temperature calculations performed by considering pro-meso and pro-racemo addition barriers at different temperatures have shown the preference for syndiotacticity which increased via decrease in temperature.

The stereospecificity in free radical polymerization of DMAAm in the presence or absence of tartrates was expected to be induced by the conformational limitations around the propagating chain which is caused by steric repulsions of amide moieties and tartrates through H-bonding interactions [17]. Hydrogen bonding is an important interaction and many times utilized to achieve the control of stereospecifity of acrylamide derivative monomers free

radical polymerizations [21–23,72–77]. Our calculations also show that the addition mode is directed by steric effects of propagating chain end and the incoming monomer and the presence of H-bondings stabilize these conformations.

6. MphAAm

Monomer structure is known to affect the stereospecific radical polymerization of vinyl type monomers [10,13]. Reactivity of alkenes is highly dependent on the pendant group size and the nature of the substituents due to the steric and polar effects. The effect of *N*-substituent of the monomer on the stereoregularity of free radical polymerization of acrylamides [18,24] have been shown.

In an experimental work [18] free radical polymerization of MphAAm was conducted in toluene at temperatures between 0 °C and −80 °C. In this study, by making use of the same model, stereoselective propagation reactions were investigated for MPhAAm. The most stable geometries of MPhAAm monomer and the corresponding radicalic model were calculated. The MPhAAm monomer has predominantly the *syn* conformation (Fig. 12). The *anti* geometry creates a steric hindrance between the phenyl ring and the C=C part of the monomer, increasing the energy by 3.60 kcal/mol in its minimum conformer. The other *anti* and *syn* conformers are much higher in energy.

The radicalic analog of the *syn* conformation is the global minimum as well and the lowest energy *anti* conformer is 4.56 kcal/mol higher in energy than that of *syn*. In all of the conformers of both monomeric and radicalic MPhAAm, H-bonding interactions are present. The pro-racemo and pro-meso additions were modeled with the *syn* conformer of monomer to account on the stereospecificity of its polymer. The most stable pro-racemo and pro-meso additions have MphAAm-ts-syn-1 and MphAAm-ts-iso-1 as transition state structures, respectively (Fig. 13) where both configurations adopt gauche conformation of the backbone.

If the trans conformation were adapted, bulky phenyl groups of the monomer and the radical would overlap on each other, giving instability to the system (Fig. 14). In the pro-racemo addition, the $C(C{=}O)NR_2$ fragments are gauche to each other. While this creates a steric hindrance between these groups, on the other hand, new stabilizing H-bondings between the carbonyl oxygens and the hydrogens at *ortho* position of phenyl group (at 2.31 Å and 2.42 Å) are formed, compensating for this steric hindrance. In the pro-meso transition state there is only one such interaction (2.47 Å). Despite the steric hindrance in pro-racemo transition state structure, the almost equal energies of both types of addition could be attributed to the extra stabilizing effect of the hydrogen bondings in MphAAm-ts-syn-1. Additionally, among the lowest pro-racemo and pro-meso transition state structures, MphAAm-ts-syn-1 has got the lowest dipole moment (1.45 D). In both MphAAm-ts-syn-1 and MphAAm-ts-iso-1 structures, the effective H-bondings are between the carbonyl oxygens and *ortho* H of phenyl groups. In the second lowest energy transition structures (MphAAm-ts-syn-2 and MphAAm-ts-iso-2) (Fig. 13) there is one H-bonding interaction in each structure at 2.54 Å and 2.51 Å in MphAAm-ts-syn-2 and MphAAm-ts-iso-2, respectively. The nature of H-bonding is different in the case of MphAAm-ts-syn-2, where the interaction is between the oxygen and H on methylene group of the monomeric radical.

Gas phase calculations do not show a distinct preference for pro-racemo or pro-meso addition for *N*-methyl-*N*-phenylacrylamide (m:r ratio of 46:54, by taking distribution of transition states), contrary to the experimental m:r ratio of 30:70 at 0 °C. However, the solvent calculations in toluene creates a better distinction, such that

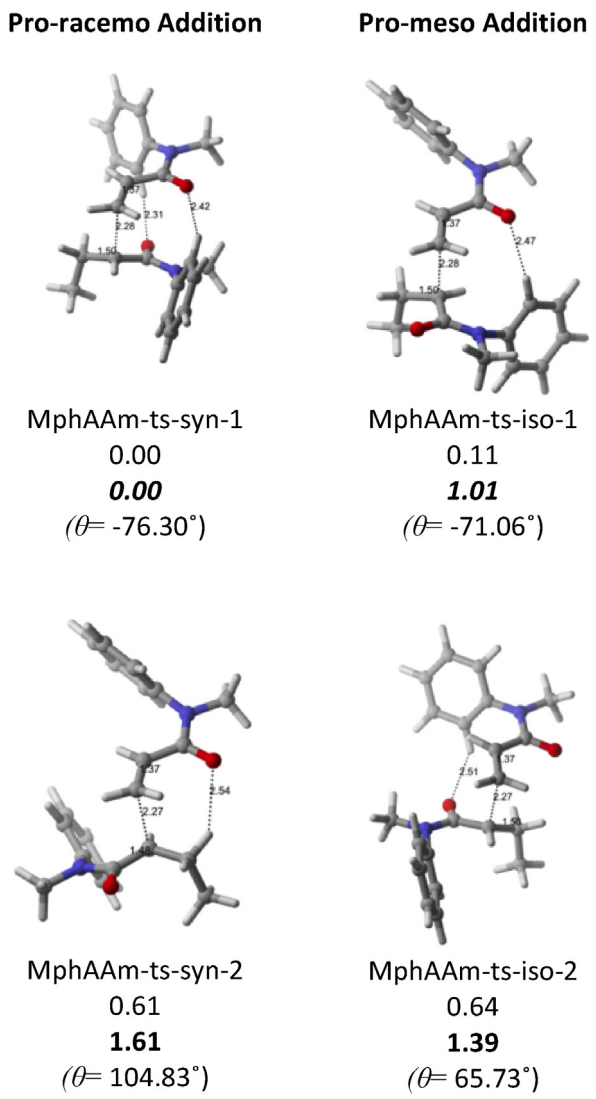

Fig. 13. The transition state structures for pro-racemo and pro-meso additions of MphAAm (the relative free energies are in kcal/mol; relative electronic energies in toluene are given in bold in kcal/mol).

the calculated m:r ratio taking the four possible transition states into account becomes 18:82, refining the quantitative trend as well.

7. DPAAm

N,*N*-Diphenylacrylamide is a good example to see how the bulkiness of a monomer has an influence on constituting a polymer configuration in terms of stereoselectivity. Possessing two bulky phenyl groups in the monomer structure, it is expected that the addition mode of this monomer is determined by these phenyl groups on steric hindrance ground.

Free radical polymerization of DPAAm is found to yield highly syndiotactic polymers regardless of the reaction conditions [19,78]. Various solvents including toluene, THF, 2-propanol, DMF and fluoroalcohols are tested within these experimental works but only a slight difference between the content of r dyad in the polymer was observed when these different solvents are used in the reaction medium especially at high temperatures.

It was shown by experiment [17] and our calculations that isotactic polymer is favored in the case of free radical polymerization of DMAAm, whereas replacing methyl groups by bulky phenyl groups causes syndiotactic polymers from DPAAm. In the last part

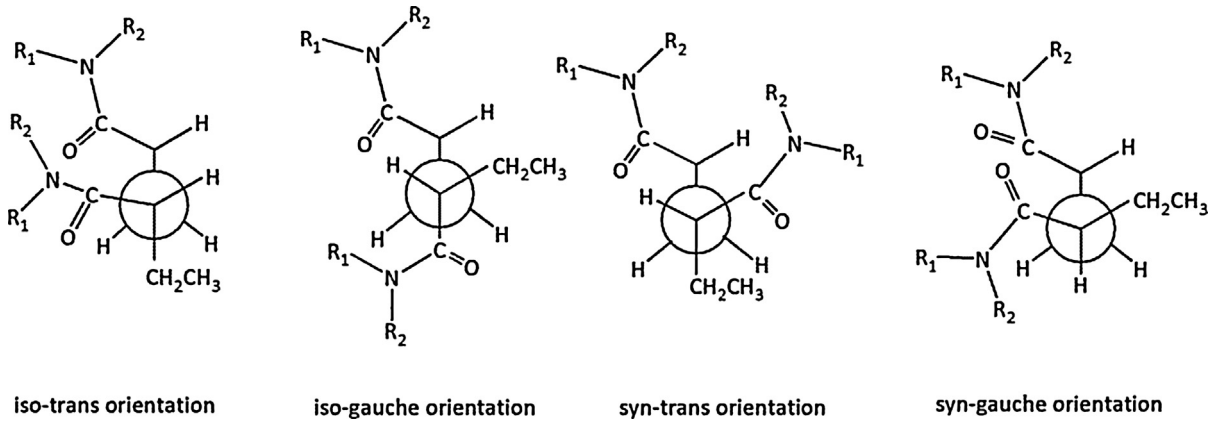

Fig. 14. The orientation of the backbone in the free radical polymerization of the monomers.

of this study, the stereoselectivity with DPAAm monomer and the effect of the two phenyl groups on propagation step of polymerization is searched.

As in DMAAm and MPhAAm monomers, the most stable monomer and the monomeric radical are the *syn* configurations. Since the energies of *anti* conformers are much higher than that of *syn*, the propagation reactions were modeled with the *syn* conformers (Fig. 15).

In the *syn* configuration, the olefinic carbons, carbonyl group and the lone pair on nitrogen are coplanar, allowing an efficient electron delocalization. The H-bonding interaction between the oxygen and the ortho H further stabilize this geometry (2.52 Å). In the *anti* geometry, the planarity is distorted and the H-bonding is weakened (2.71 Å). In their radical counterparts, the same interactions are preserved.

In the pro-racemo addition, the lowest energy transition state is DPAAm-ts-syn-1 (Fig. 16) where the geometry is similar to

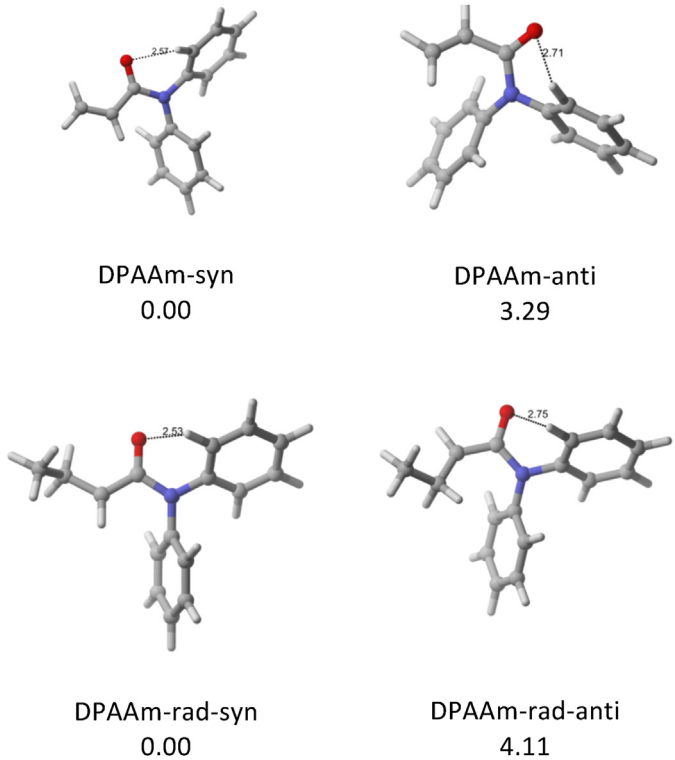

Fig. 15. The most stable conformers of DPAAm monomer and its radical (the relative free energies are in kcal/mol).

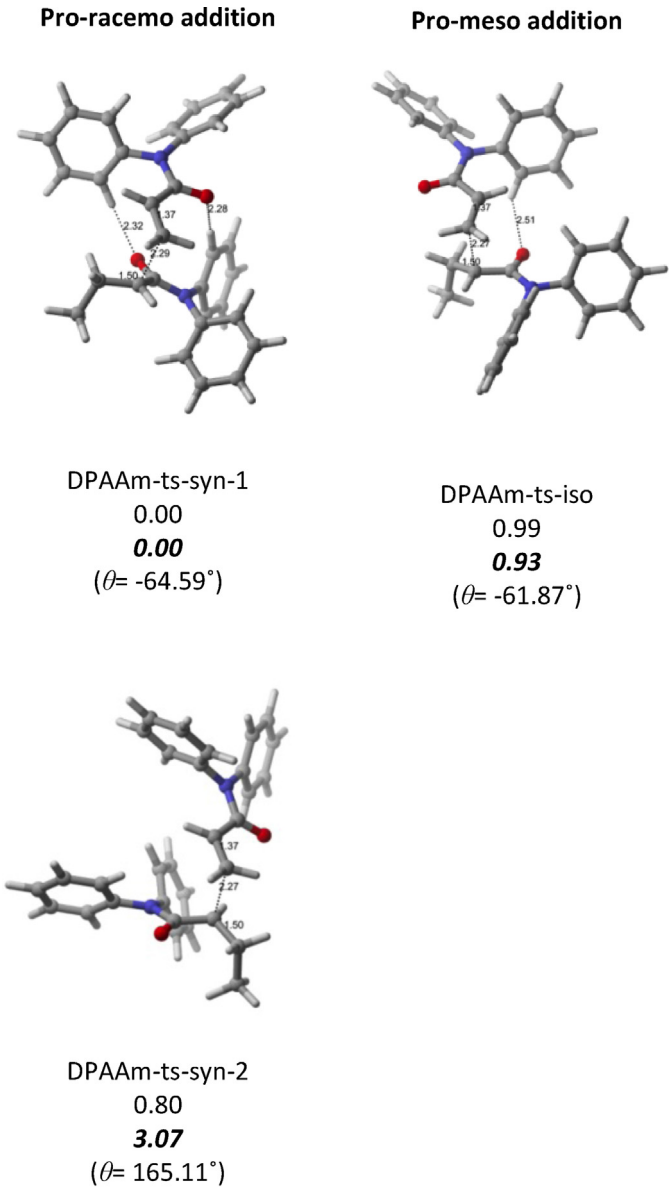

Fig. 16. The transition state structures for pro-racemo and pro-meso additions of DPAAm (the relative free energies are in kcal/mol; the relative electronic energies in toluene are given in bold in kcal/mol).

Table 3
Level of theory calculations with various functionals on B3LYP/6-31+G(d,p) geometries.

	m:r			
	DMAAm	DMAAm + tartrate	MphAAm	DPAAm
Experimental m:r ratio at 0 °C	62:38	46:54	30:70	18:82
BMK/6-311+G(3df,2p)//B3LYP/6-31+G(d,p)	92:8	23:77	0:100	8:92
MPWB1K/6-311+G(3df,2p)//B3LYP/6-31+G(d,p)	93:7	18:82	0:100	31:69
M05-2X/6-311+G(3df,2p)//B3LYP/6-31+G(d,p)	87:13	6:94	0:100	18:82
M06-2X/6-311+G(3df,2p)//B3LYP/6-31+G(d,p)	87:13	7:93	0:100	22:78
MP2/6-311+G(3df,2p)//B3LYP/6-31+G(d,p)	65:35	3:97	0:100	2:98
B3LYP/6-31+G(d,p)	86:1481:19[a]	24:76 38:62[a]	3:9746:54[a]18:82[b]	5:9512:88[a]15:85[b]

[a] From $\Delta(\Delta G)_{s\text{-}i}$.
[b] From single point IEFPCM calculations in toluene.

MPhAAM-ts-syn-1 such that, only a phenyl groups is added in the place of methyl in MphAAm-ts-syn-1. The pro-racemo transition state adopts a gauche orientation ($\theta = -64.6°$). As in MphAAm-ts-syn-1 oxygen is making two very effective inter-fragment H-bondings (2.280 Å and 2.32 Å). In the energetically higher second pro-racemo transition state (DPAAm-ts-syn-2) there is no H-bonding between the fragments, since the oxygens are oriented outwards where there is no possibility of interacting with the phenyl hydrogens. Additionally, in this geometry, the 4 phenyl groups are located on the same side of the plane and close to each other. In the pro-meso addition, only one DPAAm-ts-iso was located within 2 kcal/mol energy range. The pro-meso transition state is very similar in geometry to pro-racemo one. The only difference is in the direction of approach of the radicalic monomer to the si- or re- face of the monomer, keeping the backbone orientation almost equal. This change causes a difference in the number of H-bondings such that in DPAAm-ts-iso there is only one interaction whereas the second oxygen is directed outwards where there is no H to interact. This increases the energy of pro-meso addition as compared to pro-racemo (Fig. 16). Our results are in agreement with the experimentally found results such that pro-racemo addition reaction barrier is lower than the pro-meso addition leading to an m:r ratio of 12:88. When corrected in solution, calculations in toluene gave 15:85 for m:r ratio, which experimentally was 18:82 at 0 °C. As in other monomers studied, solvent calculations have refined the agreement however, in this case the gas phase agreement is also considerably well reproduced.

7.1. Level of theory calculations

In order to see the effect of functional a series of single point calculations have been performed with various functionals which were stated to refine the energetics for likewise systems considered in this study (Table 3) [11,31,40–48]. In B3LYP/6-31+G(d,p) calculations, the relative electronic energies for MphAAm were 0.00 and 3.61 kcal/mol for pro-racemo and 2.25 and 2.51 kcal/mol for pro-meso transition states. Inclusion of entropy have enabled both pro-racemo and meso addition modes to be almost equally probable. Although the m:r ratios with the employed functionals in Table 3 are 0:100, the entropic contribution is expected to change the ratio as in B3LYP since the single point energy differences are in 3.31–4.69 kcal/mol range. Reoptimizing the lowest energy pro-meso and pro-racemo geometries of DMAAm monomer from B3LYP/6-31+G(d,p) with M06-2X/6-311+G(3df,2p) has yielded an m:r ratio of 60:40, calculated from free energies of activation. The benchmark calculations demonstrate that the energies from different functionals are either in line with the experimental m:r ratios or with the B3LYP electronic energies which were refined by entropic corrections or by solvent corrections.

8. Conclusion

In this study, the stereoselective radical propagation reactions of *N*,*N*-dimethylacrylamide (DMAAm), *N*-methyl-*N*-phenylacrylamide (MphAAm) and *N*,*N*-diphenylacrylamide (DPAAm) monomers have been focused in their free radical polymerization. All the possible addition modes of these monomers in their propagation step of free radical polymerization have been considered with model reactions to account on their stereospecificity with quantum chemical tools. In our modeling study, all the considered monomers preferred gauche addition with $\theta \approx -70°$ in their pro-meso and pro-racemo addition modes except that of DMAAM in its pro-racemo addition. In the literature gauche orientation was reported to be the favored mode of attack in pro-meso additions, as has been observed in this study as well (Fig. 14). In the pro-racemo addition, DMAAm preferred trans conformation where DPAAm and MPhAAm preferred gauche. The trans orientation does not cause significant steric effects when the substituent is not bulky (methyl group in DMAAm) but when the phenyl groups are incorporated, the favorable H-bondings in the gauche orientation and the unfavorable steric repulsions in trans geometry enforce gauche orientation. In the preference of meso vs racemo, intramolecular H-bondings dominate such that among the most stable mode of additions, the one that permits more effective and higher number of H-bondings dominate the stereospecificity. Substitution of phenyl group(s) allows very effective H-bondings between the ortho H's and the oxygen, which stabilize pro-racemo addition mode more as compared to pro-meso. Thus, in determination of stereospecificity there is a complex interplay between the steric effects and H-bondings.

The presence of tartrate on stereospecifity has also been considered. The tartrate as tacticity inducer has changed the addition orientation in DMAAm. Although gauche orientation is preferred without tartrates in pro-meso addition, the presence of tartrates enforces a synperiplanar conformation. In pro-racemo case, trans preference was conserved. In the transition states, the preserved monomer–tartrate interactions in addition to the new ones that form between the tartrate and the incoming monomer do affect the relative energies of the transition states such that the transition structure in which tartrate is making H-bonding(s) with the new monomer is preferred over the ones that do not have.

The calculations in general have reproduced the experimental m:r preference. The solvent calculations have further refined the trends quantitatively. The calculations herein could reproduce the experimentally observed relationship between the solvent polarity and the tacticity such that increasing the polarity caused decrease in the isotacticity in DMAAm. Although the solvent methodology employed here do not consider specific solute-solvent interactions, the calculated m:r ratio reflected the experimental trend (Table 2). Furthermore, the quantitative trend has also improved by taking solvent into consideration. The level of theory calculations with

various DFT functionals has shown similar trends with either experiment or B3LYP electronic energies.

Acknowledgements

We acknowledge the National Center for High Performance Computing of Turkey (*UHEM*) under Grant 10982010; *TUBITAK ULAKBIM*, High Performance and Grid Computing Center (TRUBA resources) for computer resources provided and İstanbul Technical University Research Fund, *BAP* (30492), for supporting this study.

Appendix A. Supplementary data

Supplementary data associated with this article can be found, in the online version, at http://dx.doi.org/10.1016/j.jmgm.2014.01.005.

References

[1] M.L. Coote, T.P. Davis, L. Radom, J. Mol. Struct.: THEOCHEM 461–462 (1999) 91–96.
[2] M.L. Coote, T.P. Davis, Macromolecules 32 (1999) 2935–2940.
[3] E.I. Izgorodina, M.L. Coote, Chem. Phys. 324 (2006) 96–110.
[4] C.Y. Lin, E.I. Izgorodina, M.L. Coote, Macromolecules 43 (2010) 553–560.
[5] H. Fischer, L. Radom, Macromol. Symp. 182 (2002) 1–14.
[6] J.P. Heuts, R.G. Gilbert, L. Radom, J. Phys. Chem. 100 (1996) 18997–19006.
[7] M.W. Wong, L. Radom, J. Phys. Chem. A 102 (1998) 2237–2245.
[8] M.W. Wong, A. Pross, L. Radom, J. Am. Chem. Soc. 116 (1994) 11938–11943.
[9] X. Yu, J. Pfaendtner, L.J. Broadbelt, J. Phys. Chem. A 112 (2008) 6772–6782.
[10] İ. Değirmenci, D. Avcı, V. Aviyente, K.V. Cauter, V.V. Speybroeck, M. Waroquier, Macromolecules 40 (2007) 9590–9602.
[11] B.D. Sterck, R. Vaneerdeweg, F.D. Prez, M. Waroquier, V.V. Speybroeck, Macromolecules 43 (2010) 827–836.
[12] S.C. Thickett, R.G. Gilbert, Polymer 45 (2004) 6993–6999.
[13] İ. Degirmenci, V. Aviyente, V.V. Speybroeck, M. Waroquier, Macromolecules 42 (2009) 3033–3041.
[14] İ. Değirmenci, Ş. Eren, B.S. Sterck, K. Hemelsoet, V.V. Speybroeck, M. Waroquier, Macromolecules 43 (2010) 5602–5610.
[15] T.F. Özaltın, İ. Degirmenci, V. Aviyente, C. Atılgan, B.D. Sterck, V.V. Speybroeck, M. Waroquier, Polymer 52 (2011) 5503–5512.
[16] İ. Değirmenci, T.F. Ozaltın, O. Karahan, V.V. Speybroeck, M. Waroquier, V. Aviyente, J. Polym. Sci. Part A: Polym. Chem. 51 (2013) 2024–2034.
[17] T. Hirano, S. Masuda, S. Nasu, K. Ute, T. Sato, J. Polym. Sci. Part A: Polym. Chem. 47 (2009) 1192–1203.
[18] T. Hirano, S. Nasu, A. Morikami, K. Ute, J. Polym. Sci. Part A: Polym. Chem. 47 (2009) 6534–6539.
[19] W. Liu, T. Nakano, Y. Okamoto, Polym. J. 32 (2000) 771–777.
[20] Y. Okamoto, S. Habaue, Y. Isobe, T. Nakano, Macromol. Symp. 183 (2002) 83–88.
[21] T. Hirano, H. Ishızu, T. Sato, Polymer 49 (2008) 438–445.
[22] T. Hirano, S. Ishıı, H. Kitajima, M. Seno, T. Sato, J. Polym. Sci. Part A: Polym. Chem. 43 (2005) 50–62.
[23] T. Hirano, Y. Okumura, M. Seno, T. Sato, Eur. Polym. J. 42 (2006) 2114–2124.
[24] T. Hirano, H. Ishizu, R. Yamaoka, K. Ute, T. Sato, Polymer 50 (2009) 3522–3527.
[25] M.J. Frisch, G.W. Trucks, H.B. Schlegel, G.E. Scuseria, M.A. Robb, J.R. Cheeseman, G. Scalmani, V. Barone, B. Mennucci, G.A. Petersson, H. Nakatsuji, M. Caricato, X. Li, H.P. Hratchian, A.F. Izmaylov, J. Bloino, G. Zheng, J.L. Sonnenberg, M. Hada, M. Ehara, K. Toyota, R. Fukuda, J. Hasegawa, M. Ishida, T. Nakajima, Y. Honda, O. Kitao, H. Nakai, T. Vreven, J.A. Montgomery Jr., J.E. Peralta, F. Ogliaro, M. Bearpark, J.J. Heyd, E. Brothers, K.N. Kudin, V.N. Staroverov, R. Kobayashi, J. Normand, K. Raghavachari, A. Rendell, J.C. Burant, S.S. Iyengar, J. Tomasi, M. Cossi, N. Rega, J.M. Millam, M. Klene, J.E. Knox, J.B. Cross, V. Bakken, C. Adamo, J. Jaramillo, R. Gomperts, R.E. Stratmann, O. Yazyev, A.J. Austin, R. Cammi, C. Pomelli, J.W. Ochterski, R.L. Martin, K. Morokuma, V.G. Zakrzewski, G.A. Voth, P. Salvador, J.J. Dannenberg, S. Dapprich, A.D. Daniels, O. Farkas, J.B. Foresman, J.V. Ortiz, J. Cioslowski, D.J. Fox, Gaussian Inc., Wallingford, CT, 2009.
[26] M.L. Coote, Macromol. Theory Simul. 18 (2009) 338–400.
[27] M. Dossi, G. Storti, D. Moscatelli, Macromol. Theory Simul. 19 (2010) 170–178.
[28] D. Moscatelli, C. Cavalloti, M. Morbidelli, Macromolecules 39 (2006) 9641–9653.
[29] D. Moscatelli, M. Dossi, C. Cavalloti, G. Storti, Macromol. Symp. 259 (2007) 337–347.
[30] D. Cuccato, M. Dossi, D. Moscatelli, G. Storti, Macromol. Symp. 302 (2011) 100–109.
[31] K.V. Cauter, V.V. Speybroeck, M. Waroquier, ChemPhysChem 8 (2007) 541–552.
[32] O.F. Odio, A. Martinez, R. Martinez, R.C. Otero, L.A.M. Cabrera, J. Mol. Struct. 985 (2011) 34–47.
[33] D. Moscitelli, M. Dossi, C. Cavalloti, G. Storti, J. Phys. Chem. A 115 (2011) 52–62.
[34] K. Liang, M. Dossi, D. Moscatelli, R.A. Hutchinson, Macromolecules 42 (2009) 7736–7744.
[35] M. Dossi, K. Liang, R.A. Hutchinson, D. Moscatelli, J. Phys. Chem. B 114 (2010) 4213–4222.
[36] E.I. Izgorodina, M.L. Coote, L. Radom, J. Phys. Chem. A 109 (2005) 7558–7566.
[37] Y.X. Levine, L.J. Broadbelt, Macromolecules 41 (2008) 8242–8251.
[38] K.V. Cauter, B.V. Bossche, V.V. Speybroeck, M. Waroquier, Macromolecules 40 (2007) 1321–1331.
[39] M.K. Sabbe, A.G. Vundeputte, M.F. Reyniers, V.V. Speybroeck, M. Waroquier, G.B. Marin, J. Phys. Chem. 111 (2007) 8416–8428.
[40] A.D. Boese, J.M.L. Martin, J. Chem. Phys. 121 (2004) 3405–3416.
[41] Y. Zhao, D.G. Truhlar, J. Phys. Chem. A 108 (2004) 6908–6918.
[42] Y. Zhao, N.E. Schultz, D.G. Truhlar, J. Chem. Theory Comput. 2 (2006) 364–382.
[43] Y. Zhao, D.G. Truhlar, Theoret. Chem. Acc. 120 (2008) 215–241.
[44] A.D. Boese, J.M.L. Martin, Abstracts of Papers, 229th National Meeting of the American Chemical Society, San Diego, CA, American Chemical Society, Washington, DC, 2005, p. 274-COMP.
[45] K. Hemelsoet, V.V. Speybroeck, M. Waroquier, J. Phys. Chem. A 112 (2008) 13566–13573.
[46] R.X. Yu, J. Pfaendtner, L.J. Broadbelt, J. Phys. Chem. A 41 (2008) 4528–4530.
[47] Ö. Karahan, V. Aviyente, D. Avci, H. Zijlstra, F.M. Bickelhampt, J. Polym. Sci. Part A: Polym. Chem. 51 (2013) 880–889.
[48] B. Dedeoğlu, İ. Uğur, İ. Değirmenci, V. Aviyente, B. Barçın, G. Çaylı, H.Y. Acar, Polymer 54 (2013) 5122–5132.
[49] (a) J. Thomasi, B. Menucci, E. Cance's, J. Mol. Struct.: THEOCHEM 464 (1999) 211–226;
(b) M.T. Cance's, B. Mennucci, J. Thomasi, J. Chem. Phys. 107 (1997) 3032–3041;
(c) B. Mennucci, J. Tomasi, J. Chem. Phys. 106 (1997) 5151–5158;
(d) B. Mennucci, E. Cances, J. Tomasi, J. Phys. Chem. B 101 (1997) 10506–10517.
[50] B. Dogan, S. Catak, V.V. Speybroeck, M. Waroquier, V. Aviyente, Polymer 53 (2012) 3211–3219.
[51] M. Krajnc, I. Poljansek, J. Golob, Polymer 42 (2001) 4153–4162.
[52] N.S. Tüzün, V. Aviyente, J. Phys. Chem. A 106 (2002) 8184–8190.
[53] N.S. Tüzün, V. Aviyente, K.N. Houk, J. Org. Chem. 67 (2002) 5068–5075.
[54] N.S. Tuzun, V. Aviyente, K.N. Houk, J. Org. Chem. 68 (2003) 6369–6374.
[55] N.Ş. Tüzün, V. Aviyente, Int. J. Quantum Chem. 107 (2007) 894–906.
[56] H. Günaydın, S. Salman, N.Ş. Tüzün, D. Avcı, V. Aviyente, Int. J. Quantum Chem. 103 (2005) 176–189.
[57] Ö. Karahan, M. Işık, G. Çiftçi, İ. Uğur, D. Avcı, V. Aviyente, J. Polym. Sci. Part A: Polym. Chem. 49 (2011) 2474–2483.
[58] H. Fischer, L. Radom, Angew. Chem. Int. Ed. 40 (2001) 1340–1371.
[59] İ. Uğur, F. De Vleeschouwer, N.Ş. Tüzün, V. Aviyente, P. Geerlings, S. Liu, P.W. Ayers, F. De Proft, J. Phys. Chem. A 113 (2009) 8704–8711.
[60] N.Ş. Tüzün, V. Aviyente, D. Avcı, N. İnce, J. Mol. Model. 7 (2001) 257–264.
[61] O. Vogl, M.F. Qin, A. Zilkha, Prog. Polym. Sci. 24 (1999) 1481–1525.
[62] A.S.R. Duarte, A.M. Amorim da Costa, A.M. Amado, J. Mol. Struct.: THEOCHEM 723 (2005) 63–68.
[63] U. Berg, N. Bladh, J. Comput. Chem. 17 (1996) 396–408.
[64] M.L. Coote, T.P. Davis, Macromolecules 32 (1999) 5270–5276.
[65] M. Koyama, T. Hirano, K. Ohno, Y. Katsumoto, J. Phys. Chem. B 112 (2008) 10854–011086.
[66] Y. Katsumoto, T. Tanaka, H. Sato, Y. Ozaki, J. Phys. Chem. A 106 (2002) 3429–3435.
[67] Y. Katsumoto, N. Kubosaki, T. Miyata, J. Phys. Chem. B 114 (2010) 13312–81331.
[68] K. Satoh, M. Kamigaito, Chem. Rev. 109 (2009) 5120–5156.
[69] T. Hirano, S. Masuda, T. Sato, J. Polym. Sci. Part A: Polym. Chem. 46 (2008) 3145–3149.
[70] P.L. Polavarapu, C.S. Ewig, T. Chandramouly, J. Am. Chem. Soc. 109 (1987) 7382–7386.
[71] T. Buffeteau, L. Ducasse, A. Brizard, I. Huc, R. Oda, J. Phys. Chem. A 108 (2004) 4080–4086.
[72] T. Hirano, T. Kamikubo, Y. Okumura, T. Sato, Polymer 48 (2007) 4921–4925.
[73] T. Hirano, K. Nakamura, T. Kamikubo, S. Ishıı, K. Tanı, T. Morı, T. Sato, J. Polym. Sci. Part A: Polym. Chem. 46 (2008) 4575–4583.
[74] T. Hirano, Y. Okumura, H. Kitajima, M. Seno, T. Sato, J. Polym. Sci. Part A: Polym. Chem. 44 (2006) 4450–4460.
[75] D. Wan, K. Satoh, M. Kamigaito, Macromolecules 39 (2006) 6882–6886.
[76] T. Hirano, T. Kamikubo, Y. Fujioka, T. Sato, Eur. Polym. J. 44 (2008) 1053–1059.
[77] T. Hirano, T. Miyazaki, K. Ute, J. Polym. Sci. Part A: Polym. Chem. 46 (2008) 5698–5701.
[78] K. Shiohara, S. Habaue, Y. Okamoto, Polym. J. 28 (1996) 682–685.